Hexabromotricyclobutabenzene and Hexabromohexaradialene: Their Nickel-Mediated One-Pot Syntheses and Crystal Structures

Amnon Stanger,* Nissan Ashkenazi, Roland Boese,* Dieter Bläser, and Peter Stellberg

Abstract: The reaction of hexakis(dibromomethyl)benzene with $[(Bu_3P)_2Ni(COD)]$ (COD = 1,5-cyclooctadiene) in DMF at 65–70 °C yielded a mixture of the title compounds. The mixture was separated by column chromatography to yield hexabromotricyclobutabenzene (**3a**) and hexabromohexaradialene (**4**) in 24 and 16% yields, respectively. ^1H and ^{13}C NMR spectroscopy suggest that **3** is obtained as the *syn*-all-*trans* isomer **3a**, and the symmetric *anti*-all-*trans* isomer **3b** is not obtained at all. The X-ray structures of **3a** and **4** are reported. The hexaradialene **4** has a chair conformation, and deviates from planarity by 43.6°. Heat or radical impurities cause the clean transformation of **3a** to **4**.

Keywords
crystal structure · cyclobutenes · nickel · radialenes · radical reactions

Introduction

Tricyclobutabenzene (**1**) has been considered as one of the key compounds for the study of the long-debated Mills–Nixon effect.[1, 2] Although a strained compound, it does not show bond alternation. This was theoretically predicted (from ab initio calculations), and explained by the theoretical ability of the sp^3 carbon atoms to rehybridize and form curved ("banana") bonds.[3] Later, this was proven by X-ray and X–X electron-density deformation.[1] It was also predicted that some of the organometallic complexes of **1** will show bond alternation.[3]

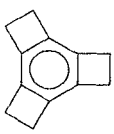

1

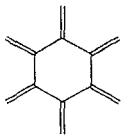

2

Synthetically, there are two multistep and low-yielding methods for the preparation of **1**;[4] no derivative of the tricyclobutabenzene skeleton is known. Thus, it was desirable to find a more efficient method for the preparation of tricyclobutabenzene, preferably a functionalized system, so that it could be used for the preparation of organometallic complexes and for organic and organometallic chemical transformations of this interesting skeleton.

The elusive hexaradialene (**2**) is a nonaromatic, ring-opened isomer of **1**. This system is of particular interest among the radialenes.[5] The parent system is unstable and polymerizes immediately.[6] Only two substituted hexaradialenes have been structurally characterized, the hexamethyl[7a] and dodecamethyl[7b] derivatives. These molecules are chair-shaped, possibly owing to the steric bulkiness of the substituents causing deviation from planarity. The question of whether **1** is more stable than **2** is still open. The interconversion between cyclobutabenzene and *o*-xylylene was investigated thoroughly,[8] and it was found that the ring-opened form is less stable (by about 8 kcal mol^{-1}) than its aromatic isomer. However, none of the reports of the synthesis of [6]-radialene (or its stable derivatives) mention conversion to the respective tricyclobutabenzene.[5, 7, 9] It may thus be that **2** is more stable than **1** (only more labile) in contrast to the cyclobutabenzene case. This can be investigated only if a synthesis of authentic tricyclobutabenzene derivatives is developed.

Our interest in the Mills–Nixon effect,[1, 3, 10] the need for functionalized cyclobutabenzenes for its study, and the general interest in compounds like **1** and **2** led us to search for an efficient method to prepare such functionalized systems. We report here the "one-pot" synthesis and the X-ray structures of the title compounds hexabromotricyclobutabenzene (**3a**) and hexabromohexaradialene (**4**),[11] and some observations regarding the interconversion of these two isomers.

Results and Discussion

As the known routes for the preparation of tricyclobutabenzene yield the unfunctionalized system (in low yields),[4] they did not fit our needs. We therefore tried our recently developed nickel-mediated cyclization method (Scheme 1),[12] in the hope that the efficiency of the reaction in closing one four-membered ring would permit the cyclization of three rings within the same

[*] Dr. A. Stanger, N. Ashkenazi
Department of Chemistry, Technion-Israel Institute of Technology
Haifa 32000 (Israel)
Fax: Int. code +(4)823-3735
e-mail: stanger@techunix.technion.ac.il
Prof. Dr. R. Boese, Dipl.-Ing. D. Bläser, Dipl.-Chem. P. Stellberg
Institut für Anorganische Chemie der Universität
Universitätsstrasse 5–7, D-45117 Essen (Germany)
Fax: Int. code +(201)183-2535
e-mail: boese@structchem.uni-essen.de

0947-6539/97/0302-0208 $ 15.00+.25/0

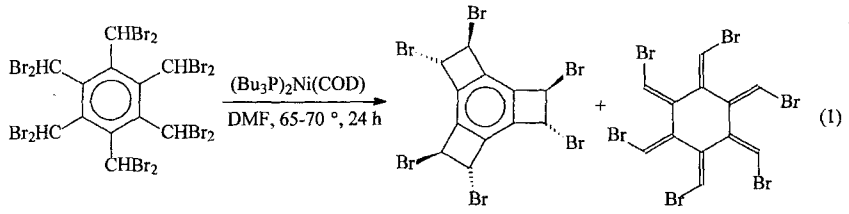

5 3a 4

Scheme 1. The attempted nickel-mediated cyclization of **5** yielded two isomers, **3a** and **4**.

molecule. The results proved to be better than expected. Three equivalents of $[(Bu_3P)_2Ni(COD)]$ (COD = 1,5-cyclooctadiene) were dissolved in dry deoxygenated DMF, hexakis(dibromomethyl)benzene (**5**)[9] was added, and the suspension stirred at 65–70 °C for 24 h. In an NMR experiment it was observed that after a few minutes at RT, before the cyclization started, the nickel complex decomposed and only free COD was present. We therefore assume that the reactive mediator is $[(Bu_3P)_2Ni(DMF)_n]$, where the complexing DMF molecules equilibrate rapidly with the solvent. The reaction takes more time than the single ring closure (24 h instead of ≈3 h[12]), probably because **5** is almost insoluble in DMF (or any other common organic solvent). The **3a**:**4** ratio in the product mixture ranges between 3:2 and 1:1, depending on exact reaction time and temperature. According to the ^1H and ^{13}C NMR spectra,[13] **3** is obtained only as the *syn*-all-*trans* isomer (**3a**). The symmetric *anti*-all-*trans* isomer (**3b**) or any of the other seven isomers that have at least one four-membered ring with a *cis* arrangement between the bromine atoms are not observed at all. The formation of the four-membered rings with only *trans* arrangement of the bromine atoms is understood on the basis of a single ring closure.[12] The sole formation of **3a** without even a trace of **3b** is probably a result of steric congestion around the *syn* bromine atom of a $CHBr_2$ unit adjacent to an already formed four-membered ring (i.e., Br_s to Br_1 and Br_2, see Scheme 2). This forces the $(Bu_3P)_2Ni$ moiety to insert into the $C-Br_a$ bond (Scheme 2), which results in a *syn* arrangement between the adjacent bromine atom on the newly formed four-membered ring and the other two. Thus, even if the first two rings were formed with an *anti* arrangement between the adjacent bromine atoms on the two rings, the third one must be formed with a *syn* relation of its bromine atoms to those in the adjacent rings.

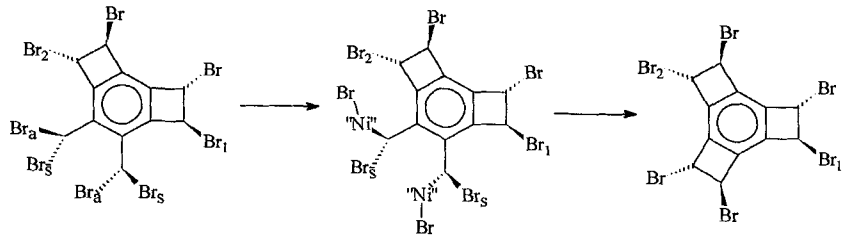

3a

Scheme 2. The formation of the third four-membered ring in **3a**. "Ni" = $(Bu_3P)_2Ni$.

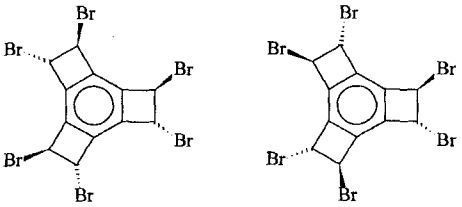

3a 3b

The workup of the reaction consists of high vacuum evaporation of the volatiles at room temperature, dissolution of the residue in chloroform, and aqueous workup. The products can be separated on an alumina column (hexane/chloroform 1:3) or by fractional crystallization (chloroform, −20 °C) to give **3** and **4** in 24 and 16% isolated yields, respectively. The mass spectrum of the mixture (CI) shows two compounds with the same molecular mass (629.4) and the same isotopic pattern (that fits $C_{12}H_6Br_6$), but with totally different fragmentation patterns. However, all the fragments are less than 8% (relative to the molecular peak).

Reacting **5** under metallic nickel cyclization conditions gave similar results; the reaction temperature needed was somewhat higher (80 °C) and the workup similar, except that the crude reaction mixture was filtered before evaporation. In this case a minor amount (3%) of a reduction product, hexakis(bromomethyl)benzene,[14] was also isolated, and the yields of **3** and **4** were 22 and 10%, respectively.

As some of the organometallic complexes that we intended to use in the Mills–Nixon effect study[3] require the parent system **1** as a precursor, we attempted the reduction of **3**. Application of the methods that were employed for the reduction of 1,2-dibromocyclobutabenzene to cyclobutabenzene (Bu_3SnCl/$LiAlH_4$[15a] or H_2 under Pd/C[15b] or Raney Ni/$NaOCH_3$ catalysis) did not yield any of the desired product **1**. Probably the presence of radicals in these reactions mediated the electrocyclic ring opening of **1** (or **3a**) to **2** that polymerized (see below).

Abstract in German: *Die Reaktion von Hexakis(dibrommethyl)benzol mit [(Bu₃P)₂Ni(COD)] (COD = 1,5-Cyclooctadien) in DMF bei 65–70 °C führte zu einem Gemisch der Titelverbindungen. Nach Säulenchromatographie wurden Hexabromtricyclobutabenzol (**3a**) und Hexabromhexaradialen (**4**) in 24 bzw. 16%-iger Ausbeute erhalten. ^1H und ^{13}C NMR-spektroskopische Daten ließen darauf schließen, daß **3** als das syn-all-trans Isomer **3a** gebildet wurde, und das symmetrische anti-all-trans Isomer **3b** nicht entstand. Die Ergebnisse aus den Röntgenstrukturanalysen von **3a** und **4** werden vorgestellt. Das Hexaradialen **4** hat Sesselkonformation mit einer Abweichung von 43.6° von der planaren Anordnung. Durch Erwärmen oder durch radikalische Verunreinigungen wird **4** glatt aus **3a** gebildet.*

However, "superhydride" ($LiEt_3BH$) successfully reduced **3a** to **1** in 54% isolated yield (i.e., 90% yield per bromine atom). Thus, the total yield from commercially available starting materials (hexamethylbenzene) to **1** is 13%, an order of magnitude higher than the yields obtained in the previously published methods.[4]

Crystals suitable for X-ray crystallography were obtained by slow crystallization of the clean compounds from chloroform at −20 °C. It was not easy to obtain the crystal structures of isomers **3a** and **4**. The molecular structure of **3a** (Figure 1) clearly reveals a conformation with C_1 symmetry, with a planar ring system. Owing to the dominant scattering of the bromine atoms, the esd's of the C–C bond distances are too high to allow a discussion of possible bond fixation, but (as expected) there are no large differences between exocyclic and endocyclic bonds.[1, 3a, 16] The molecular structure of **4** with crystallographic C_i symmetry shows that the all-*E* isomer (Figure 2, top) chair-shaped (Figure 2, bottom) conformer is formed, similar to the known hexamethyl[7a] and dodecamethyl[7b] derivatives of hexaradialene. The angle between the C(1)C(2)C(1A)C(2A) and C(2)C(3)C(1A) planes is 43.6°, that is, rather similar to the chair geometry of cyclohexane (49.3°).[17] The deviation from planarity of the substituted [6]-radialenes probably has steric and electronic causes.[18] All the other geometrical features are in the expected range.

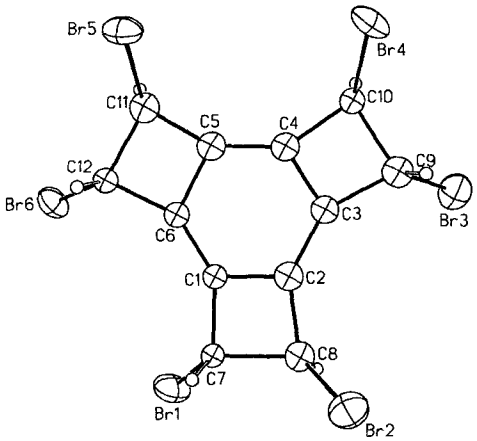

Figure 1. Ellipsoid plot of **3a**, relevant distances (Å) and angles (°): Br1 Br2 4.53, Br2–Br3 5.33, Br3–Br4 4.46, Br4–Br5 4.37, Br5–Br6 4.47, Br6–Br1 4.39; Br1-C7-C8-Br2 −126.4, Br3-C9-C10-Br4 −121.9, Br5-C11-C12-Br6 122.9.

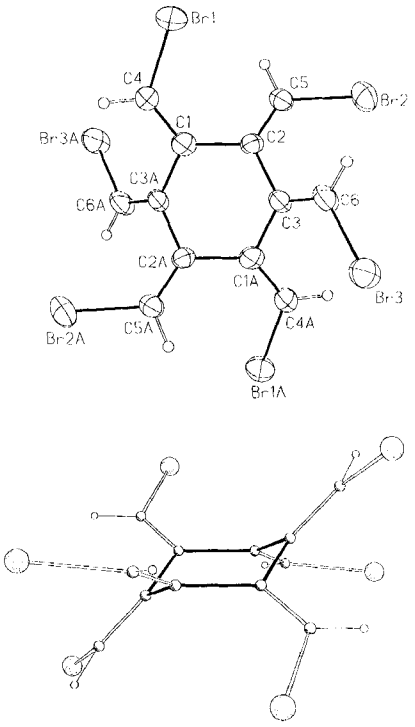

Figure 2. Ellipsoid plot of **4** (top, top view; bottom, side view); relevant distances (Å) and angles (°): C–C (ring, mean value) 1.496(7), C=C (mean value) 1.318(7), C–Br (mean value) 1.878(8); Br1–Br2 4.91, Br2–Br3 4.97, Br3–Br1A 4.80; C2-C1-C4-Br1 1.9, C1-C2-C5-Br2 −174.4, C2-C3-C6-Br3 173.5, C1-C2-C3-C1A 48.3.

Heating **3a** transformed it cleanly into **4**. Thus, if the reaction mixture (Scheme 1) was kept at the reaction temperature for a prolonged period, the yield of **3a** dropped and that of **4** increased. This happened also if a solution of **3a** in DMF or chloroform was heated. Moreover, when a solution of **3a** in $CDCl_3$[19] was placed in an open vial (in an attempt to crystallize the compound by slow evaporation of the solvent) beautiful clean crystals of **4** were found. A concerted ring opening of **3a** should be conrotatory, and therefore cannot lead to **4** (which is the all-*E* isomer). Thus, we believe that the transformation proceeds by a radical mechanism. Interestingly, although this transformation changes many properties of the molecule (for example, six carbon atoms that are sp^3 hybridized in **3a** are sp^2 hybridized in **4**), most of the geometrical changes are relatively small. Figure 3 shows an overlap presentation of **3a** and **4**, based on a fit of both six-membered rings. The positions of the six internal atoms deviate by an average distance of 0.21 Å, and the six external carbon and four bromine atoms reveal an average displacement of 1.12 and 1.30 Å, respectively. However, two of the bromine atom positions are relatively far from each other (average 3.36 Å) and suggest a rotation about the external C–C bonds during the **3a** to **4** transformation.

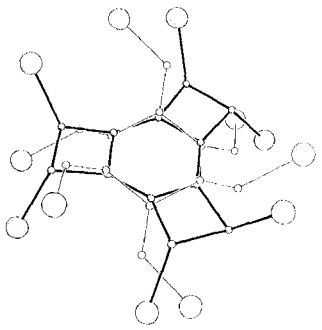

Figure 3. Overlap presentation of **3a** and **4** with best fit of the two six-membered rings.

Conclusion

The nickel-mediated cyclization of α,α,α′,α′-tetrabromo-*o*-xylene has been successfully applied to synthesize the tricyclobutabenzene skeleton. The only isomer obtained was **3a**, which can be reduced in 54% yield to the parent system **1**. The hexaradialene **4** was also obtained in this reaction, and both compounds were characterized by X-ray crystallography, which revealed no unusual structural property in these two novel systems. It was shown that **3a** cleanly transforms to **4**, probably by a radical mechanism; none of our attempts to reverse the reaction were successful. Thus, the [6]-radialene is probably thermodynamically more stable than its aromatic isomer, in contrast to what was found for the cyclobutabenzene/*o*-xylylene case. The

0947-6539/97/0302-0210 $ 15.00+.25/0 Chem. Eur. J. 1997, 3, No. 2

Methods of Calculation

Assumption of reaction pathway: In order to investigate catalysis, the substituent effect and the isotope effect, and to rationalize the complex kinetics, calculations were carried out for the respective B–V reactions of *p*-anisaldehyde and benzaldehyde with peroxyacetic acid to give *p*-anisyl- and phenylformate in nonpolar solvents. Although the B–V reaction of benzaldehyde with peroxyacid has been found mainly to give a hydride-shift compound in experiments [11–13], only the aryl migration was examined in this study, because our interest is in the substituent effect on the migratory aptitude of the aryl group. This decision was based on the grounds that the substituent effect has been found to be insensitive to variations in nonmigrating groups [11–13].

Several possible pathways for the B–V reaction were taken into consideration (Scheme 1). These pathways are based on second-order kinetics, because similar B–V reactions have been found experimentally to be second-order [9]. Because the difference in catalysis between acetic and trifluoroacetic acids has been observed experimentally for the B–V reaction of *p*-methoxyacetophenone with peroxybenzoic acid [11], catalysis with each of these acids was examined.

Several assumptions were made on the basis of the experimental findings already obtained. Firstly, we excluded from consideration the possibility of the reaction proceeding by way of an ionic species produced by the dissociation of peroxyacetic acid, because the peroxyacid is not likely to dissociate in nonpolar solvents. The experimental observation of second-order kinetics for similar B–V reactions [9] supports this assumption. Secondly, regarding the nature of acid catalysis, protonation on the carbonyl, acyloxyl, or hydroxyl oxygen was excluded from consideration, because experiments have shown that the rate of the B–V reaction of *p*-methoxyacetophenone with peroxybenzoic acid in the presence of perchloric acid in aqueous ethanol is not correlated with the acidity function H_0 but increases slightly with increasing perchloric acid content [11]. Accordingly, both acetic and trifluoroacetic acids were assumed to catalyze the reaction without apparent dissociation. Further, it was assumed that the migration in the B–V reaction occurs by a concerted mechanism, because the reaction proceeding by way of a stepwise mechanism would form unstable ionic species in nonpolar solvents. In fact, experimental results [15] support this assumption.

Ab initio molecular orbital calculation: All the geometries were optimized by the analytical gradient procedure of the GAUSSIAN92 program [16]. To select a calculation method, preliminary calculations were performed for a model reaction, the hydrogen-migratory B–V reaction of formaldehyde with peroxyformic acid, catalyzed by the hydronium ion. The geometries of the reactants and the transition state (TS) for the carbonyl addition and the migration were optimized by the use of a 3-21 G basis set at the Hartree–Fock (HF) level of theory (HF/3-21 G) and a 6-31 G* basis set at the Møller–Plesset second-order perturbation level of theory (MP2/6-31 G*). The electron energies for the HF geometries were obtained with MP2/6-31 G* (MP2/6-31 G*//HF/3-21 G). The TS geometries and their relative electron energies with respect to the reactants obtained with MP2/6-31 G*//HF/3-21 G were found to be close to those obtained with MP2/6-31 G* (Table 1). This finding indicates that the HF geometry optimization for the heteropolar dissociation of the O–O bond is acceptable, in contrast with the HF calculations for homopolar dissociation; the HF calculations provide an incorrect value of the radical dissociation energy of HOOH [17]. Although there is an energy difference of a few kcal mol^{-1} for each of the TS's between these two calculation methods, the discrepancy in the TS energy for carbonyl addition is very close to that for migration, and the comparison between the TS energies obtained with MP2/6-31 G*//HF/3-21 G for carbonyl addition and migration is then expected to provide valuable information on the mechanism of B–V reactions. Therefore, MP2/6-31 G*//HF/3-21 G was selected in the present study to reduce computational time. Considering the fact that some uncertainties associated with estimates by this calculation method could still re-

Table 1. Relative energies (kcal mol^{-1}) with respect to reactants and O–O bond lengths (Å), calculated for stationary states of the model B–V reaction with both MP2/6-31 G*//HF/3-21 G and MP2/6-31 G*.

Stationary state	MP2/6-31 G*//HF/3-21 G		MP2/6-31 G*	
	Relative energy	O–O bond length	Relative energy	O–O bond length
Reactants	0.0	1.470	0.0	1.458
TS for carbonyl addition	−43.05	1.458	−46.28	1.472
TS for migration	−39.91	1.845	−41.91	1.795
Products	−75.87	–	−76.46	–

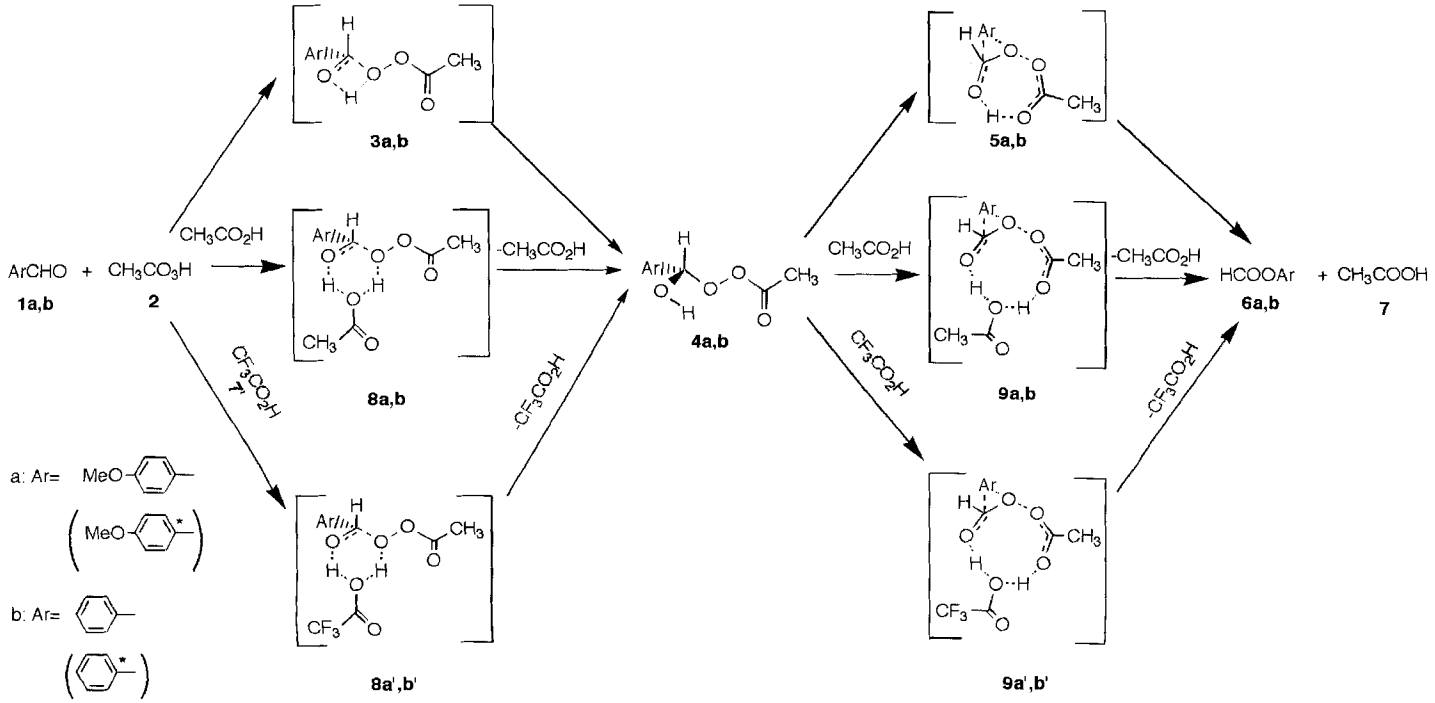

Scheme 1. Possible reaction pathways for the B–V reaction of *p*-anisaldehyde or benzaldehyde with peroxyacetic acid, either uncatalyzed or catalyzed by acetic or trifluoroacetic acid. The isotope effect was examined by the replacement of the carbon atom denoted with an asterisk by ^{14}C.

main, we will examine the complex kinetics of the B–V reactions on the basis of not only the calculation results but also the experimental facts.

Firstly, the geometries of some possible stereoisomers were optimized for several stationary states in both the B–V reactions of *p*-anisaldehyde and benzaldehyde with peroxyacetic acid by means of the minimal STO-3G basis set. The geometries at global minima on the potential-energy surface were determined so that they could serve as starting structures for the following optimizations. Secondly, the geometries were further optimized with HF/3-21G and were characterized by harmonic-frequency calculations. Finally, energy calculations for the optimized geometries were carried out; all electron energies were calculated by means of MP2/6-31G*, and then the zero-point energies and entropies and thermal energies were evaluated at 1.013×10^5 Pa and at 298 K by frequency calculations with HF/3-21G.

No isotope effect has been observed for the B–V reaction of *p*-methoxyacetophenone with *m*-chloroperoxybenzoic acid, in contrast to the decrease in reaction rate that follows an isotope substitution in other acetophenones [15]. To trace the origin of this finding, calculations were carried out for the B–V reaction in the case in which the migrating carbon atom of *p*-anisaldehyde or benzaldehyde is replaced by the corresponding isotope ^{14}C (denoted with an asterisk in Scheme 1).

Thermodynamic values in nonpolar solvents: So that we could evaluate the changes in the thermodynamic values in the liquid phase, the free-volume theory [18] was taken into consideration for estimation of the entropy difference between the gas and liquid phases. The changes in the thermodynamic values in nonpolar solvents were evaluated according to the theory with Equations (1)–(3), where ΔH_{liq}, ΔS_{liq}, and ΔG_{liq} are the changes in the

$$\Delta H_{liq} = \Delta H_{gas} - (1 - m)RT \quad (1)$$

$$\Delta S_{liq} = \Delta S_{gas} + R\ln(10^{2m\ -2}m) \quad (2)$$

$$\Delta G_{liq} = \Delta H_{liq} - T\Delta S_{liq} \quad (3)$$

enthalpy, entropy, and free energy, respectively, in nonpolar solvents, R, T, and m the gas constant, the absolute temperature, and the overall orders of reaction, respectively, and ΔH_{gas} and ΔS_{gas} the changes in the enthalpy and entropy in the gas phase that are obtained by ab initio calculations. The rate constants were evaluated according to the thermodynamic formulation of the transition state theory [18]. The tunneling effect was disregarded in the evaluation of the rate constants.

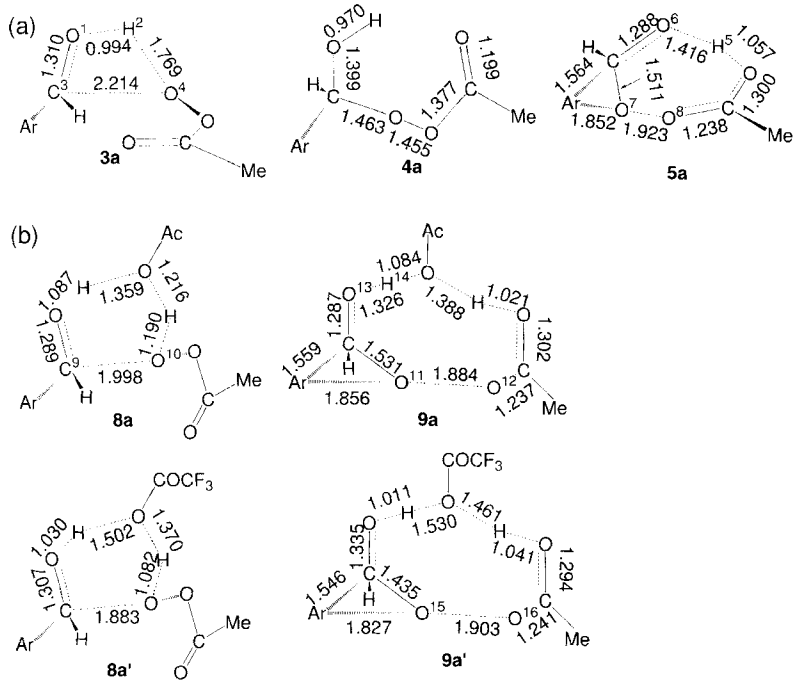

Figure 1. Optimized geometries for some important species in the B–V reactions of *p*-anisaldehyde with peroxyacetic acid: a) in the absence of acid, b) in the presence of acetic acid and of trifluoroacetic acid. The compound numbers correspond to those in Scheme 1. Numerical values for bond lengths are in Å.

Results and Discussion

Reaction mechanism in the absence of acid: Figures 1 and 2 show the optimized geometries for some important stationary states in the B–V reaction of *p*-anisaldehyde with peroxyacetic acid. The total energies and entropies are summarized in Table 2.

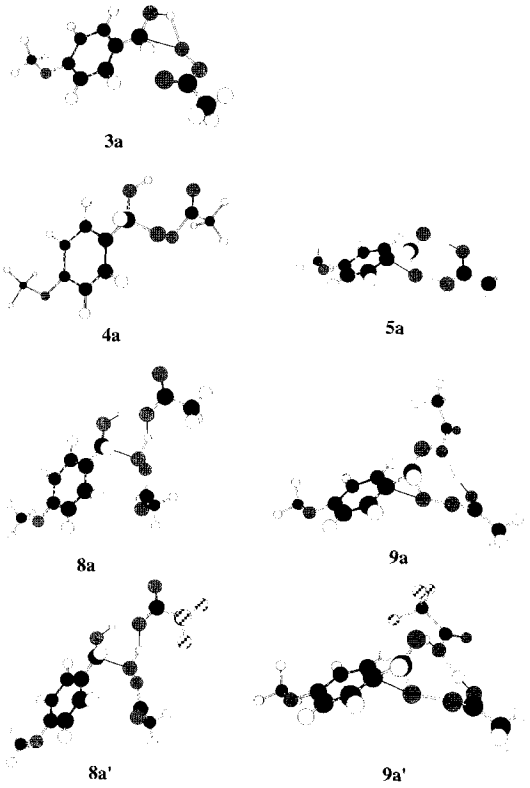

Figure 2. Cylindrical bond view of the optimized structures for the B–V reactions of *p*-anisaldehyde.

Table 2. Total energies and molar entropies at 1.013×10^5 Pa and 298 K.

Species [a]	Total energy (Hartree)	Molar entropy (cal mol^{-1} K^{-1})
1a	−458.50938	89.96
1b	−344.35862	77.49
2	−303.27824	74.36
3a	−761.72025	121.62
3b	−647.56778	109.27
4a	−761.79968	120.43
4b	−647.65023	107.72
5a	−761.74626	120.62
5b	−647.59746	107.40
6a	−533.54043	98.09
6b	−419.39178	84.81
7	−228.33648	67.30
7'	−525.42885	81.56
8a	−990.10979	152.80
8a'	−1287.20994	162.96
8b	−875.95942	139.83
8b'	−1173.05827	150.45
9a	−990.09096	151.36
9a'	−1287.21667	159.37
9b	−875.94814	138.96
9b'	−1173.06156	146.57

[a] Compound numbers correspond to those in Scheme 1.

0947-6539/97/0302-0214 $ 15.00+.25/0 Chem. Eur. J. 1997, 3, No. 2

At the TS for the carbonyl addition **3a** (Figure 1a), the distance between the carbonyl oxygen O^1 and hydroperoxyl hydrogen H^2, 0.994 Å, is seen to be quite short compared with that between the carbonyl carbon C^3 and hydroperoxyl oxygen O^4, 2.214 Å. This finding suggests that the carbonyl addition is induced by the electron-withdrawing power of the hydroperoxyl hydrogen H^2 with respect to the carbonyl oxygen O^1. Therefore, the peroxyacid should be characterized as an electrophile, and the carbonyl addition is predicted to accelerate with an increase in the electron-donating power of the migrating group. On the other hand, from comparison of the optimized structures **4a** and **5a** the migration was found to start with the cleavage of both the hydroxyl H^5–O^6 and the peroxyl O^7–O^8 bonds (Figure 1a).

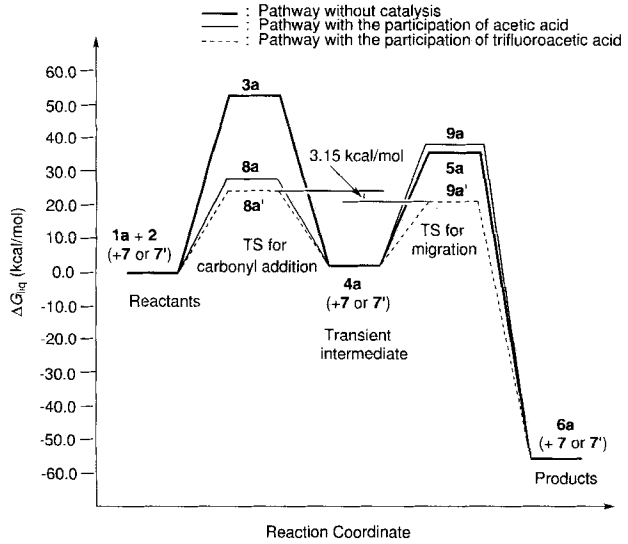

Figure 3. Schematic free-energy diagram for the B–V reaction of *p*-anisaldehyde with peroxyacetic acid in nonpolar solvents, either uncatalyzed or catalyzed by acetic or trifluoroacetic acid. The thermodynamic data for the labeled states are given in Table 3.

The energy diagram[19] (Figure 3 and Table 3) shows that the rate-determining carbonyl addition is followed by the migration, and the reaction is very exothermic. The free energy of activation for the carbonyl addition, 52.46 kcal mol^{-1}, is quite large; therefore, the reaction is expected not to occur under mild conditions. In fact, experimental results have proved that the B–V reaction is acid-catalyzed.[9, 10, 14] Even in the case of no catalyst, autocatalysis by the carboxylic acid resulting from the B–V reaction or a second peroxyacid molecule is probable. Contamination of acid in the peroxyacid should be considered if a commercial peroxyacid is used without further purification. The influence of acid on the B–V reaction should therefore be clarified to identify a rate-determining step. We excluded the autocatalysis of a second peroxyacid from consideration, because the carboxylic acid resulting from the B–V reaction should surpass the second peroxyacid in catalysis except for the initial stage of the reaction.

Reaction mechanism in the presence of acid: The distance between the carbonyl carbon C^9 and the peroxyl oxygen O^{10} in the presence of acetic acid, 1.998 Å (**8a** in Figure 1b), is seen to be shorter at the TS for the carbonyl addition than the corresponding distance in the absence of acid, 2.214 Å (**3a** in Figure 1a). The corresponding distance is further shortened by the catalysis of trifluoroacetic acid; the distance becomes 1.883 Å (**8a'** in Figure 1b). The stronger the electron-withdrawing power of the acyl group of the carboxylic acid, the shorter the distance is. These findings indicate that acid catalysis diminishes the energy of the unoccupied orbital localized mainly on the carbonyl carbon and enhances carbonyl addition. Accordingly, it is predicted that trifluoroacetic acid surpasses acetic acid in catalysis and the reactivity of the carbonyl addition in the presence of acid is superior to that in the absence of acid.

Table 3. Relative enthalpies, entropies, and free energies at 1.013×10^5 Pa and 298 K.

Species [a]	ΔH_{liq} [b] (kcal mol^{-1})	ΔS_{liq} [b] (cal mol^{-1})	ΔG_{liq} [b] (kcal mol^{-1})
3a	42.87 (42.86)	−32.17 (−32.20)	52.46 (52.46)
3b	53.50 (53.49)	−32.05 (−32.06)	53.50 (53.49)
4a	−6.98 (−7.00)	−33.49 (−33.39)	3.01 (2.96)
4b	−7.80 (−7.81)	−33.60 (−33.63)	2.22 (2.22)
5a	26.54 (26.56)	−33.17 (−33.20)	36.43 (36.46)
5b	25.31 (25.33)	−33.92 (−33.95)	35.42 (35.45)
6a	−56.03 (−56.04)	1.07 (1.07)	−56.35 (−56.36)
6b	−57.35 (−57.37)	0.26 (0.24)	−57.43 (−57.44)
8a	10.16 (10.14)	−58.34 (−58.36)	27.55 (27.54)
8a'	5.22 (5.21)	−62.44 (−62.47)	23.84 (23.84)
8b	9.91 (9.90)	−58.84 (−58.86)	27.45 (27.45)
8b'	5.79 (5.78)	−62.48 (−62.49)	24.42 (24.41)
9a	20.80 (20.81)	−59.78 (−59.79)	38.62 (38.64)
9a'	1.00 (1.00)	−66.03 (−66.06)	20.69 (20.70)
9b	16.99 (17.01)	−59.71 (−59.74)	34.79 (34.82)
9b'	3.73 (3.75)	−66.36 (−66.38)	23.52 (23.54)

[a] Compound numbers correspond to those in Figures 3 and 5. [b] The values in parentheses are those for the B–V reactions in which the migrating carbon atom of *p*-anisaldehyde or benzaldehyde is replaced by ^{14}C.

It was found that the migration in the presence of acetic acid starts with the separations of both the peroxyl O^{11}–O^{12} and hydroxyl O^{13}–H^{14} bonds (**9a** in Figure 1b), while the migration in the presence of trifluoroacetic acid starts only with the separation of the peroxyl O^{15}–O^{16} bond (**9a'** in Figure 1b). This finding means that acetic acid plays roles as both an electrophilic and a nucleophilic catalyst and the trifluoroacetic acid plays a role only as an electrophilic catalyst.

The participation of acetic acid in migration results in an unfavorable change in the activation entropy and a favorable change in the activation enthalpy. The free-energy change[19] (Figure 3) shows that the entropic disadvantage outweighs the advantage of the activation enthalpy decrease for the free energy of activation. The calculated rate constant for the migration in the presence of acetic acid (Scheme 2), $k_3^{AcOH}[AcOH] = 1 \times 10^{-12} \times [AcOH]\ s^{-1}$, was found to be smaller than the corresponding value without catalysis, $k_3^0 = 2 \times 10^{-12}\ s^{-1}$, if the concentration of acetic acid is smaller than 2 mol L^{-1}. The situ-

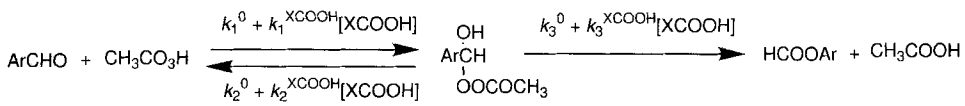

Scheme 2. Rate constants for the B–V reaction of *p*-anisaldehyde (or benzaldehyde) with peroxyacetic (or peroxytrifluoroacetic) acid.

ation is completely the reverse in the case of the carbonyl addition, and acetic acid will catalyze only the carbonyl addition and not the migration. As a whole, migration that is not acid-catalyzed was found to correspond to a rate-determining step. In approximating the overall rate constant, the transient intermediate can be assumed to be in a steady state, because the conditions of the application of the steady-state approximations discussed by Volk et al.[20] are satisfied. The apparent rate constant in the presence of acetic acid can be denoted approximately by Equation (4). It is predicted that, at a smaller con-

$$k_{\text{total}}^{\text{AcOH}} \approx \frac{k_1^{\text{AcOH}}[\text{AcOH}]k_3^0}{k_3^0 + k_2^{\text{AcOH}}[\text{AcOH}]} \quad (4)$$

centration of acetic acid, the linear relation between the rate constant and the concentration of acetic acid, $k_{\text{total}}^{\text{AcOH}} = k_1^{\text{AcOH}}[\text{AcOH}]$, is obtained and at higher concentration of acetic acid the rate constant $k_{\text{total}}^{\text{AcOH}}$ approaches the limiting value, $k_1^{\text{AcOH}}k_3^0/k_2^{\text{AcOH}}$.

The decrease in activation enthalpy owing to the participation of trifluoroacetic acid in both carbonyl addition and migration was found to be larger than that due to the participation of acetic acid. The entropic disadvantage in both the carbonyl addition and the migration is thus overcome. The calculated rate constant in the presence of trifluoroacetic acid (Scheme 2), $k_3^{\text{CF}_3\text{CO}_2\text{H}}[\text{CF}_3\text{CO}_2\text{H}] = 2\times10^1\times[\text{CF}_3\text{CO}_2\text{H}]\,\text{s}^{-1}$, is greater than the corresponding value without a catalyst, $k_3^0 = 2\times10^{-12}\,\text{s}^{-1}$ if the concentration of trifluoroacetic acid is higher than $1\times10^{-13}\,\text{mol L}^{-1}$. Not only the carbonyl addition but also the migration is catalyzed by trifluoroacetic acid, and the carbonyl addition is a rate-determining step. The apparent rate constant in the presence of trifluoroacetic acid is therefore given approximately by Equation (5) by the

$$k_{\text{total}}^{\text{CF}_3\text{CO}_2\text{H}} \approx \frac{k_1^{\text{CF}_3\text{CO}_2\text{H}}k_3^{\text{CF}_3\text{CO}_2\text{H}}}{k_2^{\text{CF}_3\text{CO}_2\text{H}} + k_3^{\text{CF}_3\text{CO}_2\text{H}}}[\text{CF}_3\text{CO}_2\text{H}] \quad (5)$$

steady-state approximation, because the conditions of application of the approximation are satisfied. The apparent rate constant is predicted to be proportional to the concentration of trifluoroacetic acid.

The relationships between the rate constant and the concentration of acid described in Equations (4) and (5) were qualitatively in good agreement with the experimental results for the B–V reaction of *p*-methoxyacetophenone with peroxybenzoic acid; specifically, the experiments showed that for catalysis with trifluoroacetic acid in benzene solvents there is a linear relationship between the rate and the concentration of acid, but catalysis with acetic acid does not show such a linear relationship.[11] Although the free-energy profile (Figure 3) might still have some uncertainties associated with energy estimates at the present calculational level, the agreement between the kinetics observed experimentally and those predicted by calculations proves the semiquantitative validity of this free-energy profile.

Therefore, we can safely say that acetic acid catalyzes only the carbonyl addition, and not migration, but trifluoroacetic acid rapidly establishes the addition equilibrium and also catalyzes the migration. It is concluded that the mechanism of the reaction varies with the catalyst.

Substituent effect: Figures 4 and 5 show the optimized geometries for some important stationary states in the B–V reaction of benzaldehyde with peroxyacetic acid. The total energies and entropies are summarized in Table 2.

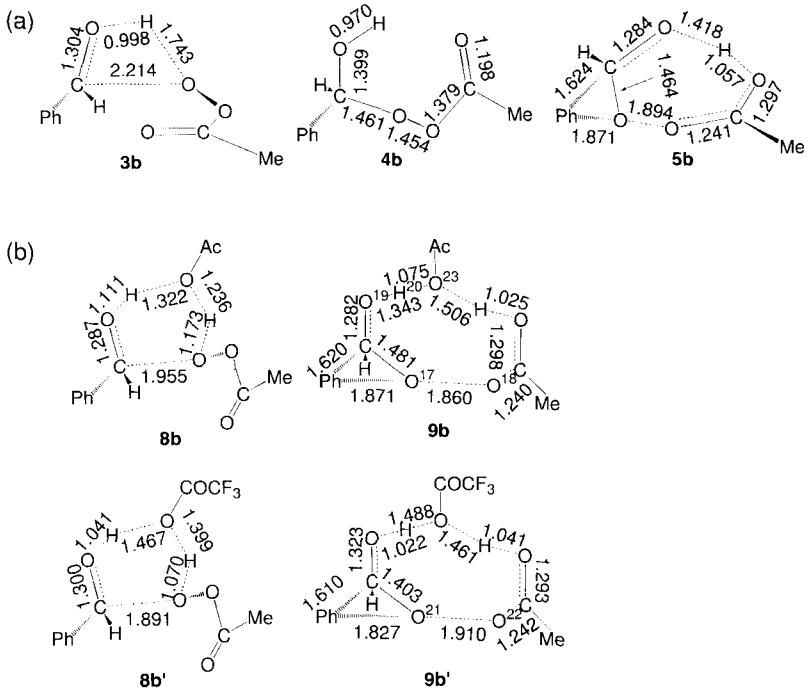

Figure 4. Optimized geometries for some important species in the B–V reaction of benzaldehyde with peroxyacetic acid; a) in the absence of catalyst, b) in the presence of acetic acid and of acid. The compound numbers correspond to those in Scheme 1. Values for bond lengths are trifluoroacetic given in Å.

The activation free energy of each of the carbonyl additions in the B–V reactions of benzaldehyde with peroxyacetic acid was found to be greater than or nearly equal to that in the case of *p*-anisaldehyde (Figures 3 and 6 and Table 3). This fact implies that the reactivity of the carbonyl addition increases with an increase in the electron-donating power of the migrating group, and the carbonyl addition is induced by the interaction between the carbonyl oxygen and the carboxyl or hydroperoxyl hydrogen.

The difference between the activation enthalpies in the absence of acid and in the presence of trifluoroacetic acid was found to be 21.58 kcal mol^{-1} for the migration in the B–V reaction of benzaldehyde with peroxyacetic acid. The difference is smaller than the corresponding difference for the migration in the B–V reaction of *p*-anisaldehyde with peroxyacetic acid, 25.54 kcal mol^{-1}. These findings indicate that the *p*-anisyl group migrates more easily than the phenyl group in the presence of trifluoroacetic acid. The situation is completely reversed in the presence of acetic acid. The activation free energy of the migration in the B–V reaction of benzaldehyde with peroxyacetic acid in the presence of acetic acid is smaller than in the case of *p*-anisaldehyde.

© VCH Verlagsgesellschaft mbH, D-69451 Weinheim, 1997 0947-6539/97/0302-0216 $ 15.00+.25/0 Chem. Eur. J. 1997, 3, No. 2

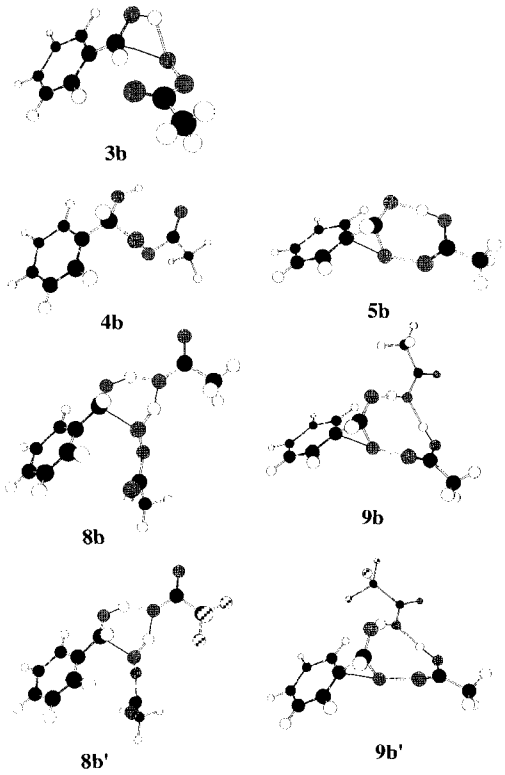

Figure 5. Cylindrical bond view of the optimized structures for the B–V reactions of benzaldehyde.

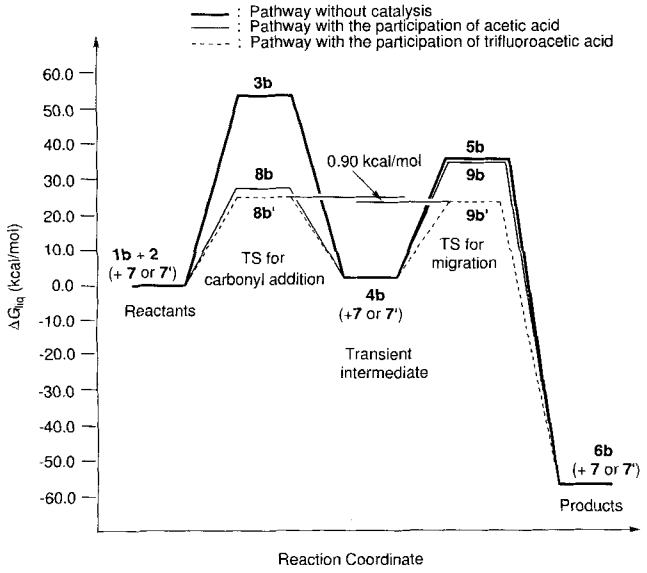

Figure 6. Schematic free-energy diagram for the B–V reaction of benzaldehyde with peroxyacetic acid in nonpolar solvents, either uncatalyzed or catalyzed by acetic or trifluoroacetic acid. The thermodynamic data for the labeled states are given in Table 3.

This fact will be explained if attention is focused on the geometrical difference in the TS for the migrations. The migration in the presence of acetic acid starts with the separations of both the peroxyl $O^{17}-O^{18}$ and hydroxyl $O^{19}-H^{20}$ bonds (**9b** in Figure 4b), but that in the presence of trifluoroacetic acid starts with the cleavage of only the peroxyl $O^{21}-O^{22}$ bond (**9b′** in Figure 4b). This situation is the same as in the case of the migration of the *p*-anisyl group. The electron donation from the carboxyl oxygen O^{23} of acetic acid to the hydroxyl hydrogen H^{20} of the carbonyl adduct intermediate leads to the separation of the hydroxyl $O^{19}-H^{20}$ bond, and this results in the migration. The migration is therefore likely to accelerate with a decrease in the electron-donating power of the migrating group. As a result, in the presence of acetic acid, the electron-donating power of the migrating group does not necessarily enhance the migration. The situation contrasts with that in the presence of trifluoroacetic acid: only the cleavage of the peroxyl $O^{21}-O^{22}$ bond induces the migration in this case (**9b′** in Figure 4b); therefore, the migration accelerates with an increase in the electron-donating power of the migrating group.

Many experiments have demonstrated the enhancement of the migration by the electron-donating power of the migrating group. This finding had been explained in terms of the stabilization of cationic intermediates. Because the B–V reactions are generally acid-catalyzed and the acids are relatively strong under the usual conditions, the migratory aptitude observed experimentally does not necessarily contradict the present calculational results. In fact, results tending to back up our calculations have been obtained for the B–V reactions of *p*-chloro- and *p*-bromobenzophenone with peroxyacetic acid in the absence of acid.[10] These reactions have been shown to yield small quantities of the products from the migration of the *p*-chloro- and *p*-bromophenyl groups, in contrast with the case in the presence of sulfuric acid, in which such products are not obtained at all. These experimental results as well as the present calculational results lead to the conclusion that migratory aptitude varies with the catalyst.

Isotope effect: It was found that the rate of migration decreases following isotope substitution of the migrating carbon by ^{14}C, and there is little isotope effect in the carbonyl addition, regardless of whether the reactant is *p*-anisaldehyde or benzaldehyde, and regardless of whether acetic or trifluoroacetic acid is used or not (Table 3). This finding indicates that the absence of an observed isotope effect for the B–V reaction of *p*-methoxyacetophenone with *m*-chloroperoxybenzoic acid is explained in terms of an exceptional rate-determining carbonyl addition.

Palmer and Fry[15] considered for the absence of any observed isotope effect that the strong electron-donating power of the *p*-methoxy group leads to a change in the force constant in the TS; the good electron-donating group causes a high density in the three-membered ring, resulting in a tight TS. The force constant in the TS at the labeled position then increases, and this results in a lowered isotope effect. On the other hand, Ogata and Sawaki[11] showed that the absence of the observed isotope effect can be attributed to a rate-determining carbonyl addition. The present result provides support for the latter view.

If attention is focused on trifluoroacetic acid catalysis, the free-energy difference between the TS for the carbonyl addition and that for the migration in the B–V reaction of *p*-anisaldehyde, 3.15 kcal mol^{-1} (Figure 3), is seen to be large compared with the corresponding difference in the case of benzaldehyde, 0.90 kcal mol^{-1} (Figure 6). In considering catalysis with an acid having electron-withdrawing power between trifluoroacetic acid and acetic acid, such as *m*-chlorobenzoic acid, it is possible that the rate-determining steps in the B–V reactions of benzaldehyde and *p*-anisaldehyde are the migration and carbonyl addition, respectively.

In the experiments of Palmer and Fry,[15] the B–V reactions of substituted acetophenones with *m*-chloroperoxybenzoic acid were carried out in the absence of acid. However, isotope effect measurements were performed for five fractions of the reactions, ranging from 8 to 60%. The autocatalysis of *m*-chlorobenzoic acid resulting from the reaction should therefore be taken into account. We suggest that the exception in the case of *p*-methoxyacetophenone is brought about by the shift of the rate-determining step from the migration to the carbonyl addition, caused by the autocatalysis.

Concluding Remarks

The mechanism of the B–V reaction of *p*-anisaldehyde with peroxyacetic acid to give *p*-anisylformate has been studied on the basis of ab initio calculations as well as experimental observations. The theoretical investigation of a rate-determining step and catalysis led to the findings that 1) the carbonyl addition corresponds to the rate-determining step in the absence of a catalyst, 2) catalysis by acetic acid contributes only to the carbonyl addition, and the rate-determining step shifts from the carbonyl addition to the migration, and 3) catalysis with trifluoroacetic acid contributes to both the carbonyl addition and migration, and the carbonyl addition corresponds to the rate-determining step. Comparison of the reaction with the B–V reaction of benzaldehyde and peroxyacetic acid to give phenylformate showed that migratory aptitude depends on catalysis. The calculational results of the isotope effect for these reactions suggested that such an effect is absent from the B–V reaction of *p*-methoxyacetophenone with *m*-chloroperoxybenzoic acid because the carbonyl addition caused by autocatalysis is the rate-determining step. These results lead to the conclusion that the B–V reaction cannot be explained in terms of only a single mechanism and the mechanism of the reaction varies with the catalyst or substituent effect.

It should be pointed out that the present investigation has been limited to the reaction in nonpolar solvents. In polar solvents or under basic conditions, the possibility of a different mechanism for the reaction, proceeding by way of ionic species, should be taken into consideration.

Acknowledgments: The author thanks Dr. M. Kagotani for his continuing support and useful suggestions from an experimental point of view. Thanks also go to Dr. H. Tsukada and Dr. M. Ohno for their reading of this paper and suggestions in its final stages.

Received: April 19, 1996 [F355]

[1] M. Hudlicky, *Oxidation in Organic Chemistry*, *ACS Monograph 186*, American Chemical Society, Washington, **1990**.
[2] R. Criegee, *Justus Liebigs Ann. Chem.* **1948**, *560*, 127.
[3] P. A. Smith in *Molecular Rearrangements*, *Vol. I* (Ed.: P. de Mayo), Interscience, New York, **1963**.
[4] J. March, *Advanced Organic Chemistry*, 4th ed., Wiley, New York, **1992**, pp. 1098.
[5] C. H. Hassall, *Org. React.* **1957**, *9*, 73.
[6] S. B. Lee, B. C. Uff, *Quart. Rev.* **1967**, *21*, 429.
[7] Y. Yukawa, T. Ando, K. Token, M. Kawada, S. Kim, *Tetrahedron Lett.* **1969**, *28*, 2367.
[8] M. A. Winnik, V. Stoute, P. Fitzgerald, *J. Am. Chem. Soc.* **1974**, *96*, 1977.
[9] S. L. Friess, A. H. Soloway, *J. Am. Chem. Soc.* **1951**, *73*, 3968.
[10] W. E. Doering, L. Speers, *J. Am. Chem. Soc.* **1950**, *72*, 5515.
[11] Y. Ogata, Y. Sawaki, *J. Org. Chem.* **1972**, *37*, 2953.
[12] Y. Ogata, Y. Sawaki, *J. Am. Chem. Soc.* **1972**, *94*, 4189.
[13] Y. Ogata, Y. Sawaki, *J. Org. Chem.* **1969**, *34*, 3985.
[14] M. F. Hawthorne, W. D. Emmons, *J. Am. Chem. Soc.* **1958**, *80*, 6398.
[15] B. W. Palmer, A. Fry, *J. Am. Chem. Soc.* **1970**, *92*, 2580.
[16] M. J. Frish, G. W. Trucks, M. Head-Gordon, P. M. W. Gill, M. W. Wong, J. B. Foresman, B. G. Johnson, H. B. Schlegel, M. A. Robb, E. S. Replogle, R. Gomperts, J. L. Andres, K. Raghavachari, J. S. Binkley, C. Gonzalez, R. L. Martin, D. J. Fox, D. J. Defrees, J. Baker, J. J. P. Stewart, J. A. Pople, *Gaussian 92, Revision A*, Gaussian, Pittsburgh, **1992**.
[17] W. J. Hehre, L. Radom, P. v. R. Schleyer, J. A. Pople, *Ab Initio Molecular Orbital Theory*, Wiley, New York, **1986**.
[18] S. W. Benson, *The Foundations of Chemical Kinetics*, Krieger, Florida, **1982**.
[19] Strictly speaking, stable complexes appear between reactants or intermediates and TSs. In fact, we obtained the optimized structures and the thermodynamic energies of these complexes and found that the free energies of several stable complexes were less than those of the corresponding precursors, that is, the reactants or intermediates. However, these stabilization energies were less than that due to the association of two acetic acids; the same is possible for the peroxyacetic acids or trifluoroacetic acids. This means that the stable complexes appearing between reactants or intermediates and TS correspond simply to the intermediate states in the overall reaction process and these will not affect the overall rate constant. Taking these facts into consideration, the free-energy diagrams in Figures 3 and 6 will be appropriate to provide essential information, even though the strict free-energy diagrams, possibly involving many molecules, may differ slightly from our diagrams; e.g., in a more strict sense, two acetic acid molecules associate with each other in the initial stage of reaction, but their influence on the relative size of the involved free-energy barriers would be negligible.
[20] L. Volk, W. Richardson, K. H. Lau, M. Hall, S. H. Lin, *J. Chem. Edu.* **1977**, *54*, 95.

0947-6539/97/0302-0218 $ 15.00+.25/0